Stub Loaded Patch Antenna and a Novel Method for Miniaturization at Sub 6 GHz 5G and Wi-Fi Frequencies

Baris Gurcan HAKANOGLU[1], Burak KOC[2], Osman SEN[3], Husnu YALDUZ[4], Mustafa TURKMEN[5,6,7]
[1]*Department of Electronics and Automation, Kirsehir Ahi Evran Unv., Kirsehir, Turkey*
[2]*Institute of Accelerator Technologies, Ankara Unv., Ankara, Turkey*
[3]*Tubitak UME, Kocaeli, Turkey*
[4]*Department of Electronics and Automation, Hitit Unv., Corum, Turkey*
[5]*Department of Electrical-Electronics Engineering, Erciyes Unv., Kayseri, Turkey*
[6]*Fotonik Technology and Engineering, Erciyes Technopark A. S., Kayseri, Turkey*
[7]*Nokta Detection Technologies R&D Center, Sancaktepe, Istanbul, Turkey*
bghakanoglu@ahievran.edu.tr

***Abstract*—This paper presents both a comprehensive analysis of a stub loaded rectangular patch antenna and a novel method to achieve more compact sizes for the antenna. It has been found that with certain stub dimensions the operating frequency shifts about 24%-27% to the lower ranges and it is possible to design the antenna with more compact sizes at these shifted bands. The model antennas are designed to operate at sub 6 GHz 5G bands and 5.8 GHz Wi-Fi band. It has been shown that the method can also be used for any frequency between 1.3 GHz and 8 GHz. Detailed parametric analyses have been performed for the best results. With these modifications, it is attained a remarkable size reduction from nearly $0.32\lambda^2$ to $0.16\lambda^2$ which means a decrease of 50% for each antenna with almost the same or better radiation characteristics. Moreover, to explain the method clearer a flow chart is given for the design procedure and to gain more confidence for our simulation results a prototype for 2.4 GHz is fabricated and measured. It has been proven that experimental measurements and simulation results are in good agreement.**

***Index Terms*—antennas, microstrip antennas, next generation networking, patch antennas, wireless LAN.**

I. INTRODUCTION

In recent years, wireless communication technology has grown so fast that today we can connect almost every device to each other without the mess of cables. This requires antennas to radiate at exact frequencies at which they are designed to operate. Also, efficient antenna structures with low losses are needed at both receiving and sending points. Microstrip patch antennas are widely used today at different frequency ranges because of low cost, easy fabrication, and compatibility with other integrated circuits. Patch antennas can be in any shape but due to the ease of analysis and good radiation characteristics rectangular microstrip antennas are used more often. When designing a rectangular microstrip antenna (RMA) it is important to tune the resonant frequency accurately, which is directly related to the input impedance of the antenna. However, because of the narrow bandwidth of the RMAs their input impedances are very sensitive to fabrication errors and substrate material characteristics [1]. So, adding tuning stubs to the structure has been an easy way to control the frequency at which the antenna operates. Additionally, phase shift and type of the polarization can be controlled by the stubs as well [2-5]. Besides attaching tuning stub elements to radiating patch to obtain multi band characteristics [6-8] a U-shaped open stub has been proposed for wireless local area network (WLAN) and ultra-wideband (UWB) operations [9]. Open ended stubs are also used in harmonic suppression of microstrip antenna [10]. In a dual-band rectangular patch antenna tuning stubs are used to control the ratio of the resonant frequencies [11]. Tuning the frequency with stubs is also used in a monopole patch antenna for dual band and WLAN operations [12-13], furthermore, it has been shown that bandwidth enhancement can be achieved by a tuning stub in a printed dipole antenna [14]. Tuning the antennas is not performed only by attaching them stubs but also it can be achieved by adding varactors, pin diodes and microelectromechanical systems (MEMS) capacitors, which ensures multiband antenna operation for tuning as well [15-19]. Another way to tune the antennas are adding metamaterials or few-layers of graphene to the stub by which the antenna can be made to operate in multiband and tuned in wide frequency ranges [20-21]. Moreover, a metamaterial substrate is introduced for both tuning and miniaturization of the antenna [22].

All the studies mentioned above have used the stubs for specific purposes and they have addressed the detailed effects of the stubs only in a few analyses. However, there are studies which clearly explain how the patch antennas react to the loaded stubs and the different values of the stub parameters. The stub loaded microstrip antennas were analyzed using generalized Thevenin theorem [23-24]. Because the mutual coupling between the patch current and the surface current on the stub should be considered an approach to calculate the surface currents on the patch together with the loaded stub is given. So, it was possible to understand the variation of the input impedance of the microstrip antenna depending on the different values of length of the stub [25]. Moreover, loading the patch antenna with one stub result in an asymmetrical current distribution. Therefore, it was presented an antenna with two stubs to

Digital Object Identifier 10.4316/AECE.2021.02003

make the current distribution symmetrical thereby improving the cross-polarization level [26]. In addition, the effects of the stub length and its width on dual band response of a rectangular microstrip antenna are presented. It was observed that the stub modifies the higher order orthogonal TM_{02} mode and fundamental TM_{10} mode resonance frequencies. Also, surface current distributions, radiation pattern and the resonance curve plots are studied [27]. Instead of using one stub, three stubs can be used to tune the frequency of the patch antenna, however, this will increase the coupling between the stubs and additional frequencies can be excited. As a solution etching slots are proposed between the stubs and etched slots making it possible to tune the antenna in desired ranges with reasonable radiation characteristics [28]. Although these studies analyze the effects of the stubs in detail and present the frequency results, they do not propose any design for the shifted bands.

This study proposes a novel method to achieve more compact sizes for the antenna without compromising the important features for the radiation. The antenna models are designed for operating at sub 6 GHz 5G bands [28] and 5.8 Wi-Fi (Wireless Fidelity) band. To improve the return loss levels and bandwidth of the stub loaded antenna additional stubs are loaded on the bottom corners of the radiating edge and a rectangular shaped slot is etched into the top stub. With these modifications, we attain a remarkable size reduction from nearly $0.32\lambda^2$ to $0.16\lambda^2$ which means a decrease of 50% for each antenna with almost the same or better radiation characteristics. The outline of the paper is as follows; Section II presents the design methodology of the reference antenna and detailed parametric analyses of the stub loaded antenna. The detailed information about the proposed model is discussed in Section III. Section IV presents the experimental results and comparison with the simulation results. Finally, Section V concludes the paper.

II. Design

The design process starts with the decision on the choice of the operating frequency of the antenna and dielectric material. Throughout the process we will design four models which are denoted by Antenna #1, Antenna #2, Antenna #3, and Antenna #4. Also, we have Antenna #0 which stands for the comparison with our proposed model operating at the desired frequency. The conventional RMA denoted by Antenna #1, which presents also the first step of the proposed design procedure is designed using the transmission line model of the patch antenna [29]. FR4 is used for the substrate of the antenna, which has a dielectric permittivity of ε_r=4.4, height of h=1.524 mm and dielectric loss tangent of δ=0.025. Fig. 1 presents the perspective view of traditional patch antenna.

There are no certain rules for the ground plane length and width. We design the ground plane dimensions according to the rule of thumb that is the distance between the ground plane edges and the edges of the radiating patch should not be less than a quarter wavelength [30]. So, for the antenna model we take dimension of the ground plane by adding quarter wavelength distance from the patch edges.

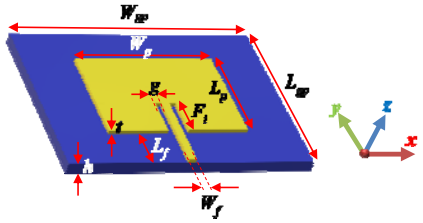

Figure 1. Presentation of the design parameters

The radiating part is modelled as a lossy conductor and its thickness is set to 0.035 mm. The feeding is performed through a microstrip feed line, which has a width of W_f and a length of L_f together with an inset feeding part with the dimensions of the length F_i and the width g. For the design W_f is taken as 3 mm for fabrication and impedance matching conditions for 50 ohms SMA (SubMiniature version A) connector. To match 50 ohms the width of the inset feeding, g is calculated together with W_f, h and ε_r. The length of inset feeding, F_i is obtained through parametric sweep analyses until we have the lowest S_{11} levels. The optimized parameters of the antenna are summarized in Table I where f_r (Antenna #0) shows the target frequency and f_r (Antenna #1) shows the frequency of the first step of the proposed design procedure which will be explained in detail in the next sections.

Table I. The Optimized Parameters of the Antenna #1

Antenna parameters	Value	Unit
f_r (Antenna #0)	2.40	GHz
f_r (Antenna #1)	3.50	GHz
ε_r	4.40	-
h	1.52	mm
Patch length, L_p	20.02	mm
Patch width, W_p	26.06	mm
Patch thickness, t	0.035	mm
Ground plane length, L_{gp}	36.57	mm
Ground plane width, W_{gp}	47.46	mm
Inset feed line length, F_i	8.20	mm
Inset feed line width, g	0.14	mm
Microstrip feed line length, L_f	7.77	mm
Microstrip feed line width, W_f	3.00	mm

According to the above results the Antenna #1 is modelled using Computer Simulation Technology Microwave Studio (CST MWS) [31]. The simulation results are displayed in Fig. 2.

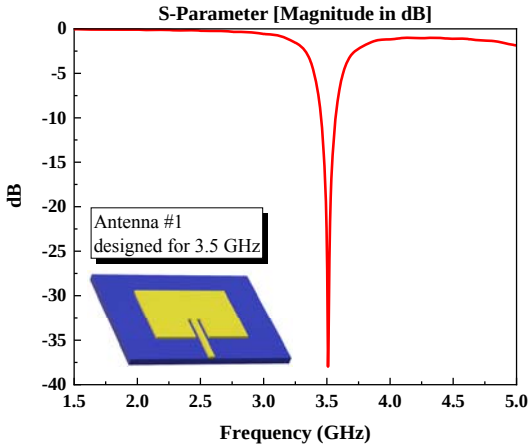

Figure 2. Antenna #1 frequency response for 3.5 GHz

The antenna designed for 3.5 GHz resonates at 3.5085 GHz with a return loss level of -37.971 dB and has a

directivity of 6.148 dBi. We will take these values as the initial states and compare to the models with tuning stubs in the next sections. To obtain the effects of the tuning stub we place a rectangular shaped stub at the center of the top edge of the antenna. Fig. 3 shows the modified antenna model denoted by Antenna #2. Parameter stub_length indicates the length of the stub in the y-direction and parameter stub_width indicates the width of the stub in x-direction. The variation of these stub parameters affects the radiation characteristics of the antenna and we will perform a detailed parametric analysis about the stub parameters.

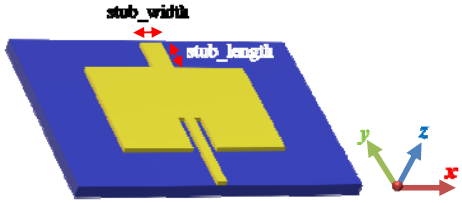

Figure 3. Antenna #2 with rectangular shaped stub loaded at the top radiating edge

In previous studies, it was stated that the stub can offer a capacitive impedance for the frequencies lower than the patch resonant frequency and inductive impedance for the frequencies higher than the patch resonant frequency when the length of the stub is nearly equal to a quarter of the wavelength on the radiating edge [27], [32-33]. In the present work, to obtain the effects of other length values of the stub and to relate the stub dimensions with antenna sizes we select the parameters stub_width and stub_length beginning with $W_p/50$ and $L_p/50$, respectively. Then for the parametric analysis we choose three other values such as $5W_p/50$, $15W_p/50$ and $25W_p/50$ for the stub_width and $5L_p/50$, $15L_p/50$ and $25L_p/50$ for the stub_length to have a clear idea of the impacts of the stub. For the parametric analysis, each time we set one parameter fixed at the chosen value and change the other. In the next sections, we will present the effects of the change of the stub dimensions in detail.

First, we will present the effects of parameter stub_width for 3.5 GHz operating RMA. Parameter stub_width is varied from $W_p/50$ to $25W_p/50$ with steps of $n \times W_p/50$ where n is selected to be 1, 5, 15, and 25 for fixed values of stub_length. Fig. 4 presents the resonant frequency variations depending on the stub_width change.

For the low values of the parameter stub_length the increase of parameter stub_width does not affect so much both the resonant frequency shift and return loss levels. However, when the stub length becomes longer and having the values of $5L_p/50$, $15L_p/50$ and $25L_p/50$ and is closer to the end point of the dielectric then stub_width affects more and more the frequency shift and resonant frequency has shifted up to 2.52 GHz, which is almost 1 GHz shift downwards for 3.5 GHz antenna. Besides shifting the resonant frequency, the return loss levels are also affected by the increase of the parameter stub_width due to the impedance variation along the edge. While the increase of the antenna area yields to shift the frequencies downwards, the input impedance mismatch causes reflection coefficient parameters to go down into inappropriate radiation.

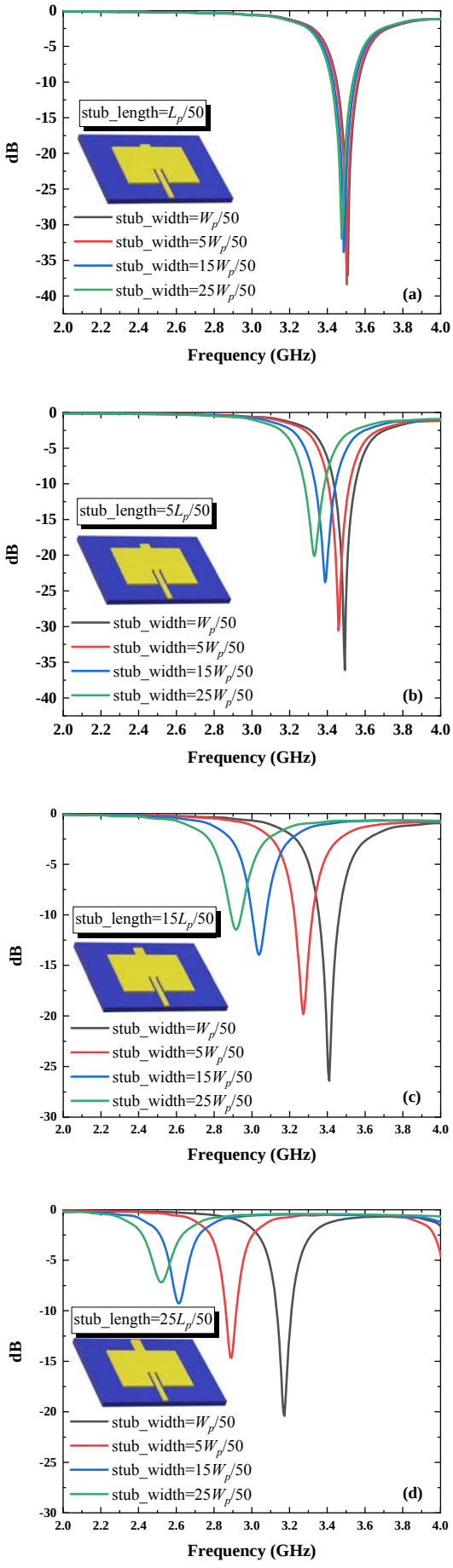

Figure 4. The effects of the parameter stub_width on resonant frequency for different values of parameter stub_length: (a) stub_length=L_p/50 (b) stub_length=5L_p/50 (c) stub_length=15L_p/50 (d) stub_length=25L_p/50

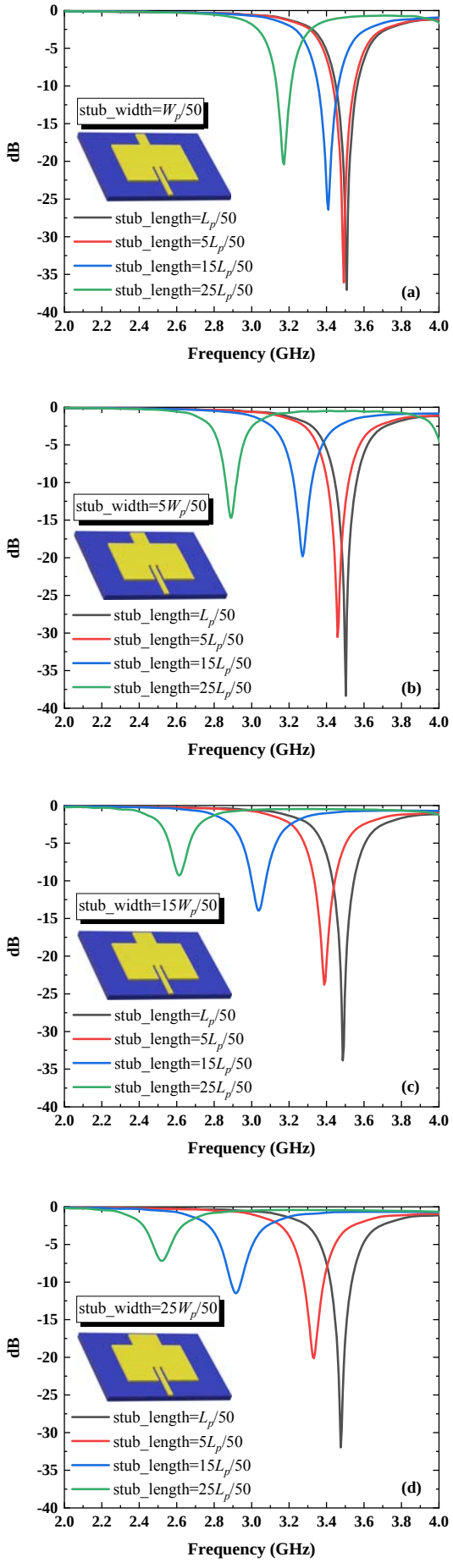

Figure 5. The effects of the parameter stub_length on resonant frequency for different values of parameter stub_width: (a) stub_width=W_p/50 (b) stub_width=5W_p/50 (c) stub_width=15W_p/50 (d) stub_width=25W_p/50

To obtain the effects of the parameter stub_length we use the same procedure which is taking L_p/50 as the starting point and increase it with the values of n×L_p/50 until it reaches the boundary of the dielectric where n=1, 5, 15, and 25 for each value of the stub_length. Fig. 5 indicates the stub_length effect on resonant frequency. For the low values of the parameter stub_width the increase of parameter stub_length does not affect so much both the resonant frequency shift and return loss levels. However, when the stub_width becomes wider and having the values of 5W_p/50, 15W_p/50, and 25W_p/50 and is closer to the end point of the patch then stub_length affects more and more the frequency. Similar to the effects of increasing the stub width, increasing the stub length decreases the reflection coefficient levels. Also, the variation of the impedance along the edge yields return loss levels decrease to lower than -10 dB. At this point we propose a method to attain impedance matching and make the return loss levels back to reasonable levels for radiation. In the next section, we present the method which makes the antenna radiate again at the shifted frequencies.

III. Proposed Model

When proper impedance matching is considered for the microstrip antennas with tuning stubs the feed position should be located on the other side of the stub and for better matching, the feed position can be moved from the y-axis position where the stub is present [28], [34]. It was displayed in the studies how the resonant frequency of a patch antenna may be adjusted by placing a tuning stub on one edge of a patch antenna with the achievable tuning dependent on the width and length of the stub and that the practical tuning range is limited by degradation of the input reflection coefficients [35-36]. Moreover, loading the antenna at one edge causes asymmetrical field distribution and high cross-polarization levels [26]. Without displacing the feed position and to make the field distribution more symmetrical, we propose two additional stubs on the corners of the bottom radiating edge. This modification will also provide the antenna improved cross-polarization levels, which will consequently increase the return loss levels. Fig. 6 shows the antenna with additional tuning stubs denoted as Antenna #3. These stubs have the same width and length with the parameter names of stub_2_width and stub_2_length, respectively.

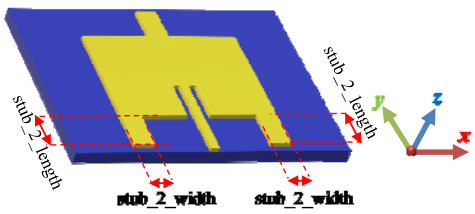

Figure 6. Antenna with additional stubs denoted as Antenna #3

With this model, four physical parameters are added by the tuning stubs at the bottom of the antenna, which are the width and the length of the stubs. Thus, the new model contains a large number of parameters that can be modified to control the operating frequency and other characteristics of the antenna. To obtain the effects of these added stubs we pick a critical return loss level of the antenna under -10 dB. From Fig. 4 (d) or Fig. 5 (c) when the stub dimensions take

the values of stub_width=15W_p/50 and stub_length=25L_p/50 the return loss level is at -9.28 dB and the antenna doesn't have reasonable radiation characteristics. For these values of the stubs the operating frequency of the antenna is 2.61 GHz, which means the stub has resulted in a frequency shift of 26% to lower region. At this point we aim the antenna to have a reasonable -10 dB bandwidth at this shifted frequency. So, we have conducted a parametric analysis about the dimensions of stub_2_width and stub_2_length. We have achieved the best return loss levels when stub_2_length is 5.6 mm and stub_2_width is 5 mm, which means stub_2_width is approximately $\lambda/8$ mm and stub_2_length is slightly longer than $\lambda/8$ mm. For the design convenience stub_2_width and stub_2_length can be taken equally, i.e., both can be $\lambda/8$ mm long. The frequency responses for different values are shown in Fig. 7 (a) and (b).

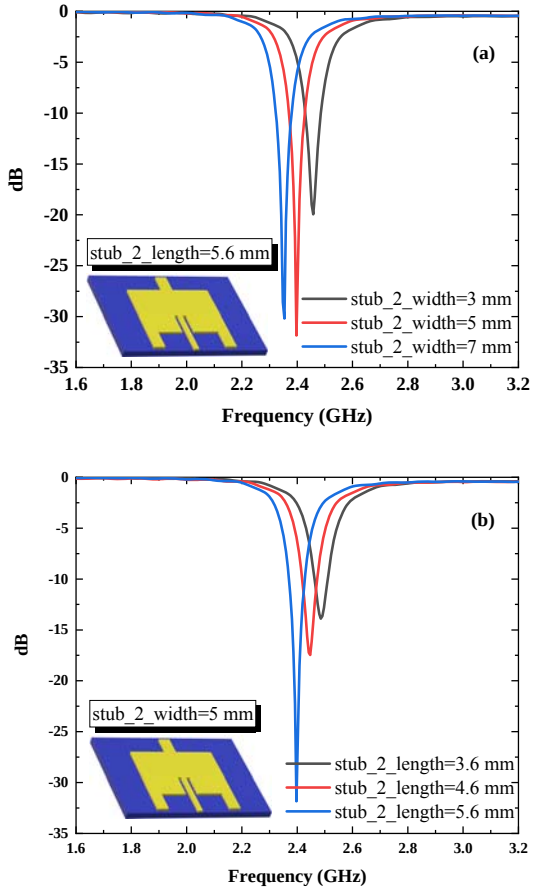

Figure 7. Frequency responses of the Antenna #3 for different (a) stub_2_width values for stub_2_length=5.6 mm, (b) stub_2_length values for stub_2_width=5 mm

Parametric analyses have been performed by changing one parameter having the other one fixed at its best value. By placing additional tuning stubs, we obtain an improved return loss of -31.85 dB, which means a 22.57 dB progress for return loss level and 56.82 MHz bandwidth improvement at 2.40 GHz. If resonance frequencies results of Antenna #2 and Antenna #3 are compared, there is a slight frequency shift from 2.61 GHz to 2.40 GHz because of the edge impedance variation, however, there is a remarkable return loss progress from -9.23 dB to -31.85 dB. Moreover, it is attained a -10 dB bandwidth enhancement from 0 MHz to 56.82 MHz.

As the final step, we embed a slot into the top stub to increase the current path and achieve additional impedance match. Fig. 8 shows the design concept of the proposed antenna denoted as Antenna #4. In addition to Antenna #3 two physical parameters are added by the slot in the top stub, which are denoted by slot_width and slot_length. To obtain the impacts of the length and width of the slot on the antenna characteristics we have performed a parametric analysis for the parameters slot_length and slot_width. Fig. 9 (a) and (b) indicate the frequency responses to the variations of the slot parameters. While the change of parameter slot_length affects the resonant frequency points, the change of parameter slot_width mainly affects the return loss levels almost for the same operating frequency.

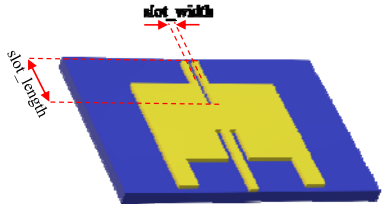

Figure 8. The proposed antenna with three tuning stubs and a slot embedded in the top tuning stub denoted as Antenna #4

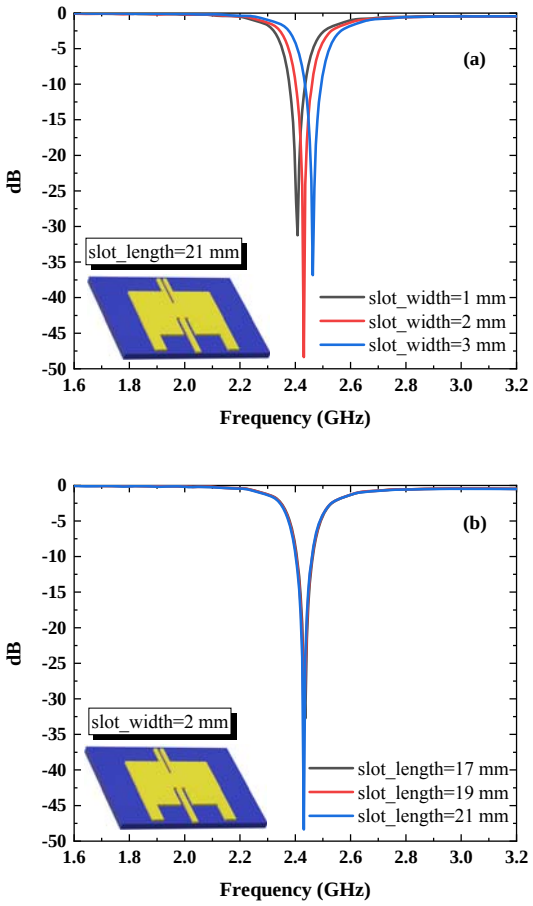

Figure 9. Frequency responses of the Antenna #4 for different (a) slot_width values for slot_length=21 mm, (b) slot_length values for slot_width=2 mm

With each design, we have obtained significant improvements in terms of return loss levels and -10 dB bandwidths. For the final design (Antenna #4), we have a return loss level -48.02 dB, which means an additional improvement of 16.17 dB compared to the Antenna #3. In

addition, the -10 dB bandwidth is 58.45 MHz, and this means that the slot has contributed with 1.63 MHz increase compared to the Antenna #3 in -10 dB bandwidth.

Fig. 10 displays the comparison of the frequency responses of all antennas, denoted as Antenna #0, #1, #2, #3, and #4. The improvement can clearly be seen from the plots.

If we summarize the results of the performed multiple parametric analyses, the design stages are carried out in accordance with the flow chart given in Fig.11. Loading the antennas with a tuning stub on the top edge with the dimensions of $25L_p/50$ and $15W_p/50$ has shifted the resonant frequencies between 24%-27% of the original frequency for each design. Table II shows further examples of the effect of the tuning stub with the dimensions of $25L_p/50$ and $15W_p/50$ for the antennas operating at frequencies between 1.3 GHz and 8 GHz.

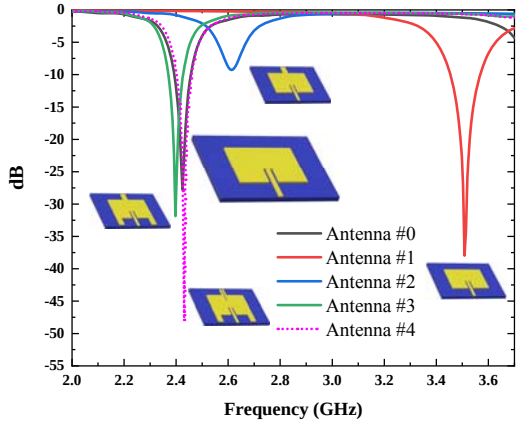

Figure 10. Comparison of the frequency responses of the Antenna #0, #1, #2, #3, and #4

So, it can be concluded that in order to have more compact structures design procedure should start to take the antenna in first step for a frequency increased by 30% from the target band. For example, if it is desired to design a compact antenna for a frequency of 5 GHz, then the starting point is to design an antenna first for 5+5×(30/100)=6.5 GHz. Next, for this frequency the rectangular antenna is designed according to the transmission line model. After that for having the frequency value at the required point, the rectangular tuning stub is loaded to the top edge of the antenna with the length of $15W_p/50$ for the width and $25L_p/50$ for the length. Because of these modifications return loss levels are not at reasonable levels so additional stubs are loaded to the bottom corners of the antenna. And for a final improvement a rectangular shaped slot is etched into the top stub by performing a short parametric analysis for the best S_{11} levels. Throughout the paper Antenna #1, #2, #3, and #4 has been compared in order to show the progress in the design stages but the main performance comparison is between Antenna #0 and #4.

To obtain the validity of the simulation results a prototype of Antenna #4 has been fabricated and measured. Vector Network Analyzer (VNA) model Anritsu 4644B (0-40 GHz) has been used for the measurements of return loss levels of Antenna #4. Fig. 12 shows the measurement setup with the fabricated antenna.

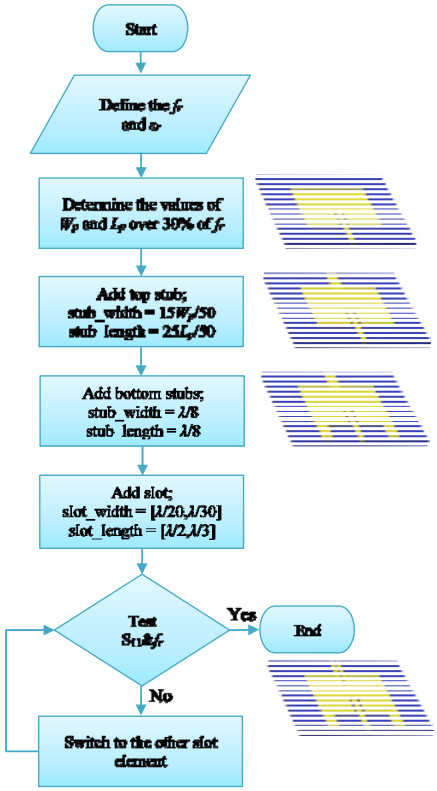

Figure 11. Flow chart of the proposed design procedure

TABLE II. VERIFICATION OF THE DESIGN STAGES FOR DIFFERENT FREQUENCIES

f_r (MHz)	Loaded stub dimensions (width×length)	f_r (MHz)	Freq. shifting (%)
1300	$15W_p/50 \times 25L_p/50$	948	27
2600	$15W_p/50 \times 25L_p/50$	1920	26
3900	$15W_p/50 \times 25L_p/50$	2924	25
5200	$15W_p/50 \times 25L_p/50$	3964	25
6640	$15W_p/50 \times 25L_p/50$	5032	24
8060	$15W_p/50 \times 25L_p/50$	6130	24

IV. EXPERIMENTAL RESULTS AND DISCUSSION

Fig. 13 presents fabricated model, Antenna #4, with dimensions. Fig. 14 shows the measured return loss levels and the simulated results together. It can clearly be seen that the measurement and simulation results agree well.

Figure 12. Measurement setup

There is a slight frequency shift. This is because of the fabrication tolerance and non-ideal conditions, which were introduced during the soldering of the SMA connector.

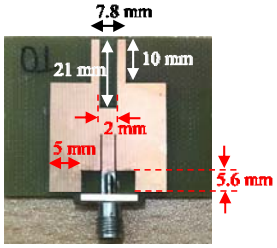

Figure 13. Parameters of Antenna #4 with dimensions

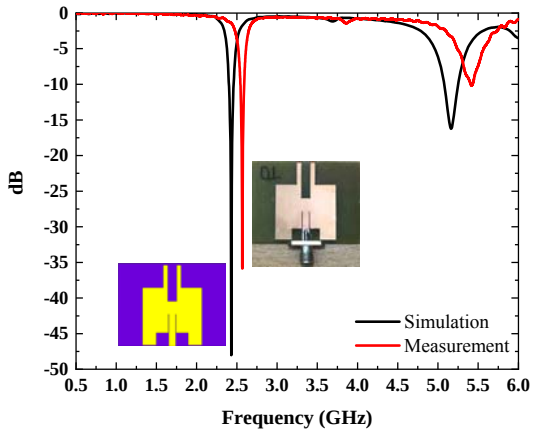

Figure 14. Comparison of the S_{11} measurement and simulation results for the Antenna #4

Fig. 15 (a) and (b) show the E-plane and H-plane radiation characteristics for Antenna#0 and Antenna#4 at 2.43 GHz, respectively. The results indicate that for E-plane, Antenna#0 has a main lobe magnitude of 6.28 dBi with 3 dB angular width of 89.7° and the main lobe magnitude for Antenna#4 is 5.16 dBi with 3 dB bandwidth of 111.2°. In addition, for H-plane Antenna#0 has a main lobe magnitude of 6.31 dBi with 3 dB angular width of 98.1° and the main lobe magnitude for Antenna#4 is 5.32 dBi with 3 dB bandwidth of 106.1°. From the figures it can clearly be concluded that with the proposed method the miniaturized antenna model can be accomplished almost with the same radiation characteristics as the original antenna.

The current distributions of Antenna #0 and Antenna #4 are presented in Fig. 16. The current distribution for Antenna #0 is distributed over the antenna surface. This current distribution on the surface does not affect the propagation characteristics of the antenna much. Thanks to the modifications applied, surface current distribution is directed to the bottom and top stubs of the antenna as it should be.

Moreover, in addition to increasing the current distribution density present at the top corners, new current distributions were created at the propagation edges corresponding to the bottom tuning stubs.

For the further validation of the present approach different models are designed for operating at 3.5 GHz, 4.7 GHz, and 5.8 GHz. FR4 is used for all models with dielectric permittivity of ε_r=4.4 as the substrate with the same height of 1.524 mm and dielectric loss tangent of δ=0.025. Also, the dimensions of the substrate are calculated using the same procedure, which is the distance between the ground plane edges and the edges of the radiating patch should not be less than a quarter wavelength [30].

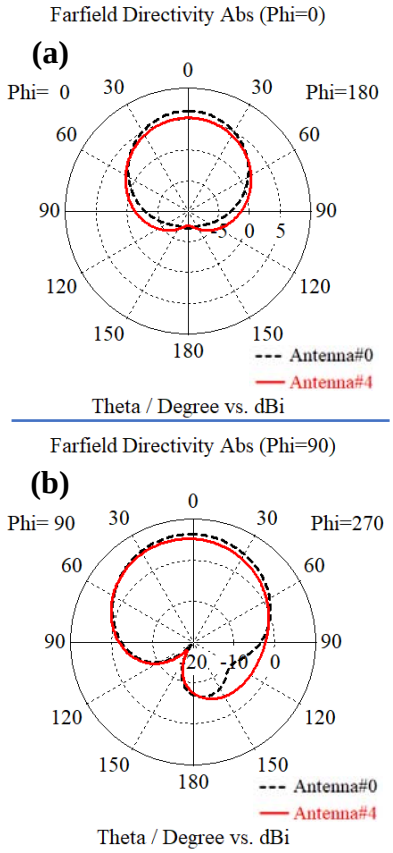

Figure 15. Simulated radiation patterns of Antenna#0 and Antenna #4 for 2.43 GHz, (a) E–plane, (b) H–plane

Each plot in Fig. 17 shows the comparisons of frequency responses of the antennas of each design step for 3.5 GHz, 4.7 GHz, and 5.8 GHz bands. For four different frequency bands, we have obtained the same effects with Antenna #4. The results are summarized in Table III.

The final models of the antennas give us also the possibility to design the structures in more compact areas. The proposed antenna operating at 2.43 GHz has a size of $W_p \times L_p$=26.06 mm×20.02 mm, however, if we design a patch antenna for 2.43 GHz then it has a size of $W_p \times L_p$=37.53 mm×29.08 mm. Similarly, the proposed antenna operating at 3.46 GHz has a size of $W_p \times L_p$=19.41 mm×14.74 mm, however, if we design a patch antenna for 3.46 GHz then it has a size of $W_p \times L_p$=26.37 mm×20.25 mm. It is obtained the same results for 4.7 and 5.8 GHz operating antennas as well.

The designed antenna is compared with the proposed miniaturized antennas exist in literature in Table IV in terms of miniaturization technique, antenna sizes, size reduction percentages, resonance frequencies, peak gains at resonance frequencies and return loss levels. In the table, it is seen that with the proposed method, a size reduction of 51%, 47%, 44% and 47% can be achieved with the antennas operating at 2.4 GHz, 3.5 GHz, 4.7 GHz and 5.8 GHz, respectively. The most important advantage of the proposed method is that the dimensions of the design parameters are associated with the wavelength studied. Thus, it has been ensured that the method is easily applicable for antennas working with different frequencies and different materials.

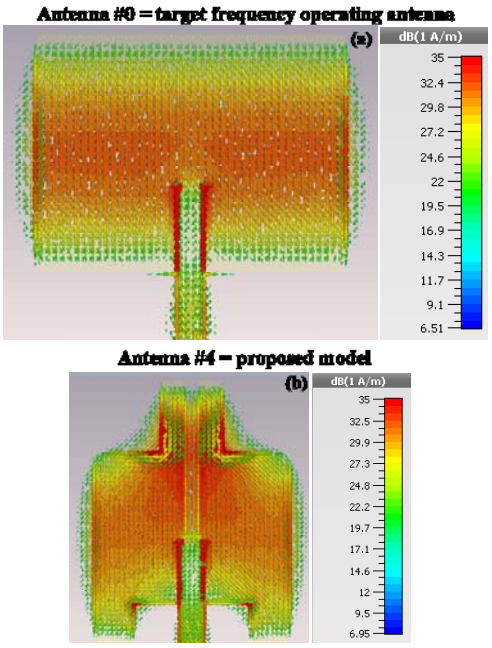

Figure 16. The current distribution of the antennas at their resonant frequencies (a) Antenna #0, (b) Antenna #4

V. Conclusion

A novel method to achieve compact designs for patch antennas is proposed and the effects of rectangular shaped tuning stubs on resonant frequencies of a rectangular patch antenna designed for 2.4 GHz, 3.5 GHz, 4.7 GHz, and 5.8 GHz have been investigated.

Loading the patch antenna with one stub has resulted in limitations about the bandwidth and return loss levels. In order to solve this problem, we have proposed additional tuning stubs loaded on the corners at the bottom radiating edge of the antenna.

Consequently, it has been achieved remarkable progress in return loss levels and bandwidth of the antenna. For additional improvements, it has been etched a rectangular shaped slot into the tuning stub on the top radiating edge.

As a result, the negative effect of one tuning stub on the return loss levels and bandwidth has been eliminated when the stub has large surface sizes.

The final model occupying smaller area is fabricated and has been shown that the fabricated antenna has almost the same results as the simulated one. For further verification, different antennas are designed for 3.5 GHz, 4.7 GHz, and 5.8 GHz.

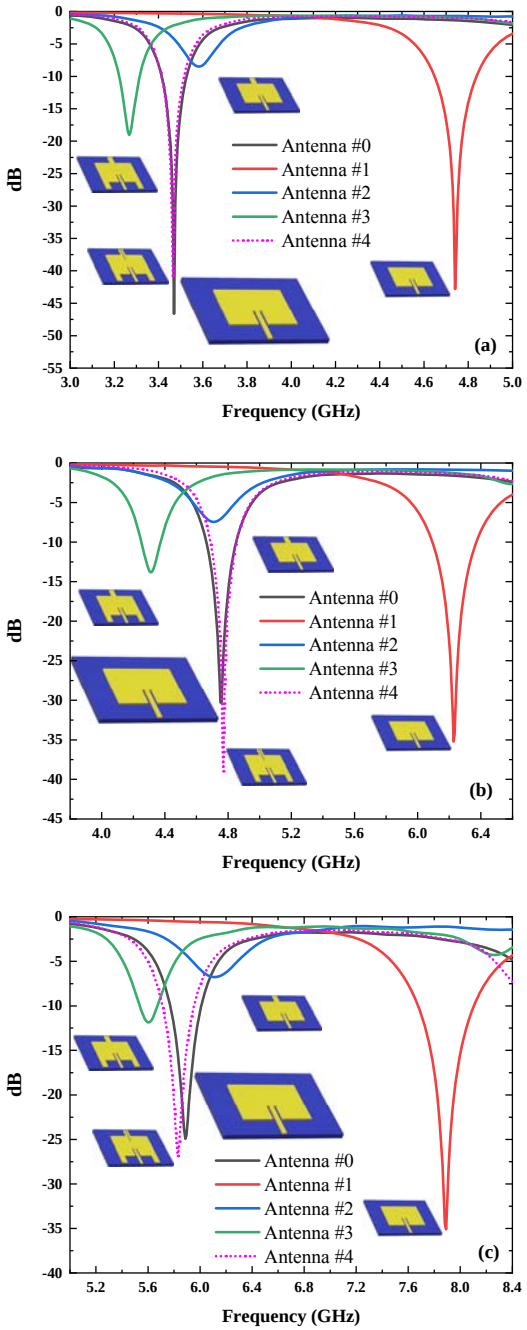

Figure 17. Further verification of our method for the patch antennas designed for (a) 3.5 GHz, (b) 4.7 GHz, and (c) 5.8 GHz

Table III. The Comparison between the Target Antennas and the Proposed Designs

Parameters	**2.4 GHz**		**3.5 GHz**		**4.7 GHz**		**5.8 GHz**	
	Ant. #0	Ant. #4	Ant. #0	Ant. #4	Ant. #0	Ant. #4	Ant. #0	Ant. #4
f_r (GHz)	2.43	2.43	3.47	3.46	4.76	4.77	5.89	5.83
S_{11} (dB)	-27.74	-48.02	-46.65	-41.14	-30.32	-38.98	-24.92	-26.94
Current Density (A/m^2)	124.3	209.1	327.4	416.4	815.4	1433	1503	2244
Elec. Energy Density (J/m^3)	0.0058	0.0116	0.0120	0.0130	0.0255	0.0489	0.0475	0.0779
Mag. Energy Density (J/m^3)	0.0180	0.0183	0.0314	0.0281	0.0742	0.0665	0.1272	0.1461
Main Lobe Magnitude (dBi)	6.31	5.32	6.15	5.38	6.21	5.56	6.36	5.59
-10 dB Bandwidth (MHz)	63.8	58.5	113.5	102.3	188.5	166.1	241.8	246.1
% Bandwidth	2.63	2.41	3.27	2.96	3.96	3.48	4.11	4.22
W_p (λ)	0.63	0.44	0.64	0.47	0.65	0.49	0.65	0.49
L_p (λ)	0.49	0.33	0.49	0.36	0.49	0.37	0.49	0.36
$W_p \times L_p$ (λ^2)	0.31	0.15	0.32	0.17	0.32	0.18	0.32	0.17
W_{gp} (mm)	68.01	47.46	48	34.81	35.51	27.44	28.88	22.33
L_{gp} (mm)	52.76	36.57	36.99	26.80	27.14	20.77	21.90	16.72
$W_{gp} \times L_{gp}$ (mm^2)	3588.21	1735.61	1775.52	932.91	963.74	569.93	632.47	373.35

TABLE IV. THE COMPARISON OF PRESENT WORK WITH THE LITERATURE

Ref.	Description	Antenna Size (mm^3)	Size Reduction	Freq. (GHz)	Gain (dBi/dB)	Return Loss (dB)
[4]	Triangular patch with a tuning stub	48×41.6×1.6	22%	1.708	-	-
[37]	Defected Ground with EBG	35×29×1.5	37.9%	2.47	4.68 dBi	-24
[38]	Ground-cut slots	37×47×2	62.3%	2.29	5.72 dB	-25
[39]	U-shaped slot	43×70×1.5	57%	0.915	4.74 dB	-
[40]	Dielectric resonator antenna using parasitic C-slot	40×40×4.9	-	2.5 5.8	4.3 dBi 3.8 dBi	-28 -18
[41]	Stepped Impedance Resonator	64×45×1	-	2.5 5.8	-1.8 dBi 1.1 dBi	-18 -19
This work	Loaded tuning stubs to radiating edges	26×20×1.5	51%	2.4	5.32 dBi	-48
	Loaded tuning stubs to radiating edges	20×15×1.5	47%	3.5	5.38 dBi	-40
	Loaded tuning stubs to radiating edges	15×11×1.5	44%	4.7	5.56 dBi	-39
	Loaded tuning stubs to radiating edges	12×8.8×1.5	47%	5.8	5.59 dBi	-27

The same procedure is applied to the antennas to have more compact size and reasonable radiation at shifted frequencies. As a result, we have achieved the same results for the improvement of return loss levels and bandwidth of the antenna at shifted frequencies.

REFERENCES

[1] M. Du Plessis, J. Cloete, "Tuning stubs for microstrip-patch antennas," IEEE Antennas Propag. Mag., vol. 36, no. 6, pp. 52-56, 1994. doi:10.1109/74.370523

[2] S. K. Roy, L. Jha, "Effects of tuning stub on microstrip patch antenna," Indian Journal of Radio&Space Physics, vol. 34, pp. 139-141, 2005

[3] Y. Sung, "Axial ratio-tuned circularly polarized square patch antenna with long stubs," Int. J. Antennas Propag., vol. 2018, 2018. doi:10.1155/2018/7068560

[4] J. H. Lu, K. L. Wong, "Single-feed circularly polarized equilateral-triangular microstrip antenna with a tuning stub," IEEE Trans. Antennas Propag., vol. 48, no. 12, pp. 1869-1872, 2000. doi:10.1109/8.901278

[5] S. A. Bokhari, J. -F. Zurcher, J. R. Mosig, F. E. Gardiol, "A small microstrip patch antenna with a convenient tuning option," IEEE Trans. Antennas Propag., vol. 44, no. 11, pp. 1521-1528, 1996. doi:10.1109/8.542077

[6] W. A. Hasan, M. M. Saleh, O. Alknbar, A. K. Jasim, A. N. Abdulfattah, M. E. Ali, "Design and fabrication of triple frequency microstrip patch antenna by attaching tuning stub element," 10th International Conference on Telecommunication Systems Services and Applications, pp. 1-4, 2016. doi:10.1109/TSSA.2016.7871064

[7] K. P. Ray, G. Kumar, "Tuneable and dual-band circular microstrip antenna with stubs," IEEE Transactions on Antennas and Propagation, vol. 48, no. 7, pp. 1036-1039, 2000. doi:10.1109/8.876321

[8] M. Koohestani, M. Golpour, "U-shaped microstrip patch antenna with novel parasitic tuning stubs for ultra wideband applications," IET Microwaves, Antennas & Propagation, vol. 4, no. 7, pp. 938-946, 2010. doi:10.1049/iet-map.2009.0049

[9] J. N. Lee, J. H. Kim, J. K. Park, J. S. Kim, "Design of dual□band antenna with u□shaped open stub for WLAN/UWB applications," Microwave and Optical Technology Letters, vol. 51, no. 2, pp. 284-289, 2009. doi:10.1002/mop.24033

[10] C. K. Ghosh, "Harmonics suppression of microstrip antenna using open ended stubs," Microwave and Optical Technology Letters, vol. 58, no. 6, pp. 1340-1345, 2016. doi:10.1002/mop.29809

[11] Jung-Hyo Kim, Jeong-Wook Lee, Jong-Gwan Yook, Han-Kyu Park, "Frequency tuning of slot-loaded rectangular patch antenna with tuning stubs and gaps," IEEE Antennas and Propagation Society International Symposium, vol. 3, pp. 298-301, 2001. doi:10.1109/APS.2001.960091

[12] L. Peng, C. L. Ruan, "A microstrip fed monopole patch antenna with three stubs for dual-band WLAN applications," Journal of Electromagnetic Waves and Applications, vol. 21, no. 15, pp. 2359-2369, 2007. doi:10.1163/156939307783134263

[13] H. Wang, "Dual-resonance monopole antenna with tuning stubs," IEE Proceedings-Microwaves, Antennas and Propagation, vol. 153, no. 4, pp. 395-399, 2006. doi:10.1049/ip-map:20050110

[14] Y. Liu, S. Gong, A. Bu, "Bandwidth enhancement of printed dipole antenna with tuning stub," Microwave and Optical Technology Letters, vol. 50, no. 10, pp. 2653-2656, 2008. doi:10.1002/mop.23718

[15] M. A. Madi, M. Al-Husseini, M. Mervat, "Frequency tunable cedar-shaped antenna for WIFI and WIMAX,", Progress In Electromagnetics Research, vol. 72, pp. 135-143, 2018. doi:10.2528/PIERL17091505

[16] S. N. M. Zainarry, N. Nguyen-Trong, C. Fumeaux, "A frequency- and pattern-reconfigurable two-element array antenna," IEEE Antennas and Wireless Propagation Letters, vol. 17, no. 4, pp. 617-620, 2018. doi:10.1109/LAWP.2018.2806355

[17] A. F. Sheta, S. F. Mahmoud, "A widely tunable compact patch antenna," IEEE Antennas and Wireless Propagation Letters, vol. 7, pp. 40-42, 2008. doi:10.1109/LAWP.2008.915796

[18] E. Erdil, K. Topalli, M. Unlu, O. A. Civi, T. Akin, "Frequency tunable microstrip patch antenna using rf mems technology," IEEE Transactions on Antennas and Propagation, vol. 55, no. 4, pp. 1193-1196, 2007. doi:10.1109/TAP.2007.893426

[19] N. Nguyen-Trong, L. Hall, C. Fumeaux, "A frequency- and polarization-reconfigurable stub-loaded microstrip patch antenna," IEEE Transactions on Antennas and Propagation, vol. 63, no. 11, pp. 5235-5240, 2015. doi:10.1109/TAP.2015.2477846

[20] T. Ali, R. C. Biradar, "A compact multiband antenna using λ/4 rectangular stub loaded with metamaterial for IEEE 802.11 N and IEEE 802.16 E," Microwave and Optical Technology Letters, vol. 59, no. 5, pp. 1000-1006, 2017. doi:10.1002/mop.30454

[21] M. Yasir, P. Savi, S. Bistarelli, A. Cataldo, M. Bozzi, L. Perregrini, S. Bellucci, "A planar antenna with voltage-controlled frequency tuning based on few-layer graphene," IEEE Antennas and Wireless Propagation Letters, vol. 16, pp. 2380-2383, 2017. doi:10.1109/LAWP.2017.2718668

[22] K. Buell, H. Mosallaei, K. Sarabandi, "A substrate for small patch antennas providing tunable miniaturization factors," IEEE Transactions on Microwave Theory and Techniques, vol. 54, no. 1, pp. 135-146, 2006. doi:10.1109/TMTT.2005.860329

[23] M. D. Deshpande, Y. R. Rao, "Technical memorandum: Analysis of reactively loaded microstrip disk antenna," IEE Proceedings H (Microwaves, Antennas and Propagation), vol. 136, no. 5, pp. 417-419, 1989. doi:10.1049/ip-h-2.1989.0074

[24] M. Bailey, "Analysis of the properties of microstrip antennas using strips embedded in a grounded dielectric slab," 1979 Antennas and Propagation Society International Symposium, pp. 370-373, 1979. doi:10.1109/APS.1979.1148143

[25] M. D. Deshpande, M. C. Bailey, "Analysis of stub loaded microstrip patch antennas," IEEE Antennas and Propagation Society International Symposium, vol. 2, pp. 610-613, 1997. doi:10.1109/APS.1997.631535

[26] A. E. Daniel, G. Kumar, "Tunable dual and triple frequency stub loaded rectangular microstrip antennas," IEEE Antennas and Propagation Society International Symposium, vol. 4, pp. 2140-2143, 1995. doi:10.1109/APS.1995.531018

[27] A. A. Deshmukh, P. Baxi, C. Kamdar, B. Vora, K. P. Ray, "Analysis of stub loaded rectangular microstrip antenna," Proceedings of National Conference on Communications (NCC), pp. 1-5, 2012

[28] M. M. Rahman, M. S. Islam, H. Y. Wong, T. Alam, M. T. Islam, "Performance analysis of a defected ground-structured antenna loaded with stub-slot for 5G communication," Sensors, vol. 19, no. 11/2634, 2019. doi:10.3390/s19112634

[29] C. A. Balanis, Antenna theory: Analysis and design, 3rd edition, pp. 816-820, John Wiley & Sons, 2005

[30] J. Huang, "The finite ground plane effect on the microstrip antenna radiation patterns," IEEE Transactions on Antennas and Propagation, vol. 31, no. 4, pp. 649-653, 1983. doi:10.1109/TAP.1983.1143108

[31] Computer simulation technology (CST) microwave studio, Ver. 2016, Framingham, MA, USA, 2016

[32] I. J. Bahl, P. Bhartia, Microstrip Antennas, pp. 203-215, Artech House, 1980

[33] R. Garg, P. Bhartia, I. J. Bahl, A. Ittiboon, "Microstrip antenna design handbook", pp. 302-311, Artech House, 2001

[34] F. R. Yang, Y. Qian, R. Coccioli, T. Itoh, "Analysis and application of photonic band-gap (PBG) structures for microwave circuits," Electromagnetics, vol. 19, no. 3, pp. 241-254, 2007. doi:10.1080/02726349908908642

[35] D. M. Pozar, "Trimming stubs for microstrip feed networks and patch antennas," IEEE Antennas and Propagation Society Newsletter, pp. 26-28, 1987

[36] D. M. Pozar, B. Kaufman, "Design considerations for low sidelobe microstrip arrays," IEEE Transactions on Antennas and Propagation, vol. 38, no. 8, pp. 1176-1185, 1990. doi:10.1109/8.56953

[37] D. Singh, A. Thakur, V. M. Srivastava, "Miniaturization and gain enhancement of microstrip patch antenna using defected ground with EBG," Journal of Communications, vol. 13, no. 12, 2018. doi:10.12720/jcm.13.12.730-736

[38] Y. Li, Y. Liu, S. Gong, "Microstrip antenna using ground-cut slots and miniaturization techniques with low RCS," Progress In Electromagnetics Research Letters, vol. 1, pp. 211-220, 2008

[39] A. Ghiotto, S. F. Cantalice, T. P. Vuong, A. Pouzin, G. Fontgalland, S. Tedjini, "Miniaturized patch antenna for the radio frequency identification of metallic objects," IEEE MTT-S International Microwave Symposium, pp. 583-586, 2008. doi:10.1109/MWSYM.2008.4633233

[40] H. Chen, Y. Wang, Y. Lin, S. Lin, S. Pan, "A compact dual-band dielectric resonator antenna using a parasitic slot," IEEE Antennas and Wireless Propagation Letters, vol. 8, pp. 173-176, 2009. doi:10.1109/LAWP.2008.2001119

[41] C. Hsieh, C. Wu, T. Ma, "A compact dual-band filtering patch antenna using step impedance resonators," IEEE Antennas and Wireless Propagation Letters, vol. 14, pp. 1056-1059, 2015. doi:10.1109/LAWP.2015.2390033